Available online at www.sciencedirect.com
ScienceDirect
Trans. Nonferrous Met. Soc. China 35(2025) 2354−2371
Transactions of Nonferrous Metals Society of China
www.tnmsc.cn

Spatial distribution and source-specific ecological risk assessment of heavy metals in surface sediments of Dongting Lake, China

Yao ZHOU[1,2,3], Yong-sheng CHENG[1,2,3]

1. Key Laboratory of Metallogenic Prediction of Nonferrous Metals and Geological Environment Monitoring, Ministry of Education, Central South University, Changsha 410083, China;
2. Hunan Key Laboratory of Nonferrous Resources and Geological Hazards Exploration, Changsha 410083, China;
3. School of Geosciences and Info-Physics, Central South University, Changsha 410083, China

Received 9 September 2024; accepted 28 April 2025

Abstract: Environmental problems from heavy metals (HMs) attract global attention. Accurately identifying sources and quantitatively evaluating ecological risks are keys for HMs pollution prevention. Dongting Lake in China was investigated through integrated methods like positive matrix factorization and Nemerow integrated risk index to examine spatial distribution, contamination characteristics, pollution sources, and the contribution of each source and pollutant to the ecological risk of 14 HMs in its surface sediments. Results showed that the mean concentrations of HMs were 0.82−9.44 times greater than the corresponding background values. The spatial distribution of HMs varied significantly, with high values of As, Cd, Mn, Pb, Sn, Tl and Zn concentrated in the sediments from Xiangjiang inlet and Yangtze outlet; Co, Cr, Cu, Ni and V in the Lishui sediments; Hg and Sb in the sediments from Yuanjiang and Zishui inlets, respectively. The accumulation of HMs was affected by five sources: mercury mining and atmospheric deposition (F1) (17.99%), urban domestic sewage and industrial sewage discharge (F2) (24.44%), antimony ore mining and smelting (F3) (6.50%), non-ferrous metal mining and extended processing industrial sources (F4) (15.72%), and mixed sources mainly from natural sources and agricultural sources (F5) (35.35%). F1 and F2 were identified as priority pollution sources; Cd, Hg, Tl, Sb and As, especially Cd and Hg, posed relatively high ecological risks and were prioritized HMs for control.

Key words: Dongting Lake; surface sediments; heavy metal pollution; source apportionment; positive matrix factorization (PMF) model; risk assessment

1 Introduction

Heavy metals (HMs) pollution from high-intensity human activities (e.g., industrialization, urbanization, and agricultural intensification) has become a global environmental issue [1,2]. HMs can enter water bodies via various channels, including wastewater discharge, industrial activities, traffic emissions, and agricultural chemicals, posing significant risks to aquatic ecosystems and human health due to their toxicity, persistence, and bioaccumulation [3−7]. Lake sediments are regarded as “storage reservoirs” of HMs, recording rich information on environmental changes in the lake area [8−12]. The concentration of HMs in lack sediments serves as a sensitive indicator for reflecting anthropogenic impacts on the lake area’s ecological environment and monitoring lake ecosystem ecological risks [4,13]. Thus, investigating the distribution characteristics, potential ecological risks, and sources of HM pollution in lake surface sediments is crucial for guiding efforts in the prevention and control of

Corresponding author: Yong-sheng CHENG, Tel: +86-13017386868, E-mail: cys968@163.com
https://doi.org/10.1016/S1003-6326(25)66820-8

environmental HMs pollution.

The sources of HMs in sediments are extensive, falling into two main categories: natural sources and anthropogenic sources. Natural sources primarily refer to HMs generated during soil formation processes, such as rock weathering. The HMs generated from these natural sources generally exhibit low concentrations and do not pose significant harm to flora and fauna or the environment [14−16]. Anthropogenic sources are the primary contributors to excessive HMs. They primarily include wastewater, waste gases and solid waste emissions from industrial and mining activities (such as those from mining, metallurgy, and electroplating industries); the use of chemical fertilizers, pesticides, and livestock and poultry breeding in agriculture; gasoline combustion, exhaust emissions, tire wear, and brake pad wear during transportation; industrial production and municipal waste from power plants, chemical plants, coal-consuming enterprises, and metallurgical industries; as well as the long-distance migration of HMs caused by atmospheric deposition [17−22]. The sources of HMs in sediments are complex, and understanding the sources and distribution of HMs is crucial for effective control of surface sediment pollution.

Principal component analysis (PCA), absolute principal component score-multiple linear regression (APCS-MLR) analysis, UNMIX, chemical mass balance (CMB), the positive matrix factorization (PMF), and isotope methods are commonly used for the source analysis of HMs in sediment [18,23−25]. Among these methods, PMF has the advantages of applying nonnegative constraints and better performance in solving factor values while considering uncertainties, making it widely used for the source analysis of pollutants in sediments [1,20,26]. In addition, GIS mapping is an effective tool for describing the spatial distribution of data sets to visualize the characteristics of heavy metals in sediments. It not only provides intuitive information on the impacts of various pollution sources but also makes important supplements and confirmations to the results of PMF model. Therefore, the combined application of PMF and GIS mapping can further promote the allocation of various pollution sources and support the contributions from different sources obtained by PMF, playing a crucial role in the regional environmental protection and pollution control. Methods such as enrichment factors (EF), potential ecological risk indices (RI), the Nemerow index, and the Geo-accumulation index (I_{geo}) [23,27−30] are often used in regional ecological risk assessment. However, these methods can only conduct comprehensive ecological risk assessment of multiple risk sources within a region, but cannot identify priority control sources or corresponding priority control pollutants. Combining quantitative source analysis models with ecological risk assessment models can both quantify the ecological risks induced by each pollution source to identify priority sources and effectively determine the HMs associated with these sources, thus contributing to precise management of regional HMs pollution.

Dongting Lake, the second-largest freshwater lake in China, is hailed as the “Kidney of the Yangtze River” [31]. There are a large number of ore deposits and towns distributed in the watersheds of the Four Rivers flowing into Dongting Lake, namely Xiangjiang (XR), Zishui (ZR), Yuanjiang (YR), and Lishui (LR) [13,26,32−35]. The extraction and subsequent exploitation of mineral resources have not only spurred rapid economic development within the watershed but have also substantially heightened the risk of HMs pollution in the environment surrounding Dongting Lake. Therefore, it is of crucial significance to thoroughly understand the characteristics of HMs pollution in the Dongting Lake watershed. However, most of the current studies on HMs pollution in Dongting Lake focus on the body of the lake [10], with relatively insufficient attention given to its major inlets and outlet. In this study, 14 HMs (As, Cd, Co, Cr, Cu, Hg, Mn, Ni, Pb, Sb, Sn, Tl, V and Zn) in the surface sediments of the Four Rivers inlets and the Yangtze River outlet of Dongting Lake were taken as the research objects. We utilized a combination of multiple methods, including multivariate statistical analysis, I_{geo}, GIS analysis, PMF and NIRI, to explore the spatial distribution characteristics, ecological risks and pollution sources of HMs in the surface sediments from Dongting Lake, and to identify the priority control pollution sources and the corresponding priority control HMs of it. This will contribute to the precise control of pollution in Dongting Lake, thus providing a solid basis for the scientific and efficient prevention of HMs pollution,

the reduction of ecological and environmental risks, as well as the safeguarding of human health.

2 Experimental

2.1 Study area

Dongting Lake (112°14′32.1″−112°56′18.3″E, 28°45′47.5″−29°11′08.1″N), with a total watershed area of 3.24×10^{11} m^2, and a lake water storage capacity of approximately 1.78×10^{11} m^3, is located in northern Hunan Province, China. Dongting Lake drains into the Yangtze River to the northeast and is fed by the Four Rivers from the northwest (Fig. 1). It is the second-largest freshwater lake across China, with important ecological functions including water regulation, fisheries, navigation, irrigation, drinking water supply, climate regulation, tourism, and biodiversity conservation [32,36,37]. The lake area has a subtropical monsoon climate, with an average annual temperature of 16−20 °C, an average precipitation of 1237−1354 mm, and an elevation range of 26−1500 m. Its land use types are dominated by cultivated, forests and construction lands; its predominant soil types are paddy soils, red soils, and fluvo-aquic soils (Fig. 2). The Four Rivers watersheds, which feeds into Dongting Lake, are characterized by widespread towns and mineral deposits. The XR watershed is the primary source of non-ferrous metals resources in Hunan Province, featuring the world's largest tungsten deposit at Shizhuyuan, as well as significant resources of tin, antimony, copper, and manganese. The watershed is highly urbanized with intensive land use [35,38]. The ZR watershed has abundant antimony reserves, accounting for 80% of the world's total [33,39,40]. The YR spans across Hunan and Guizhou province, meandering through the Tongren−Phoenix mercury mining belt. The watershed teems with mercury resources, of which the Wanshan ore field has cumulative proven mercury reserves of 2.04×10^4 t, accounting for over 60% of the country's total [41]. The Shimen realgar mine of LR watershed is the largest medicinal realgar deposit globally and also hosts a phosphorus deposit of 1.5×10^9 t [42]. The Four Rivers watersheds boast a well-developed and historically significant industry for smelting non-ferrous metals like lead and zinc, and are strategic regions for central China's development,

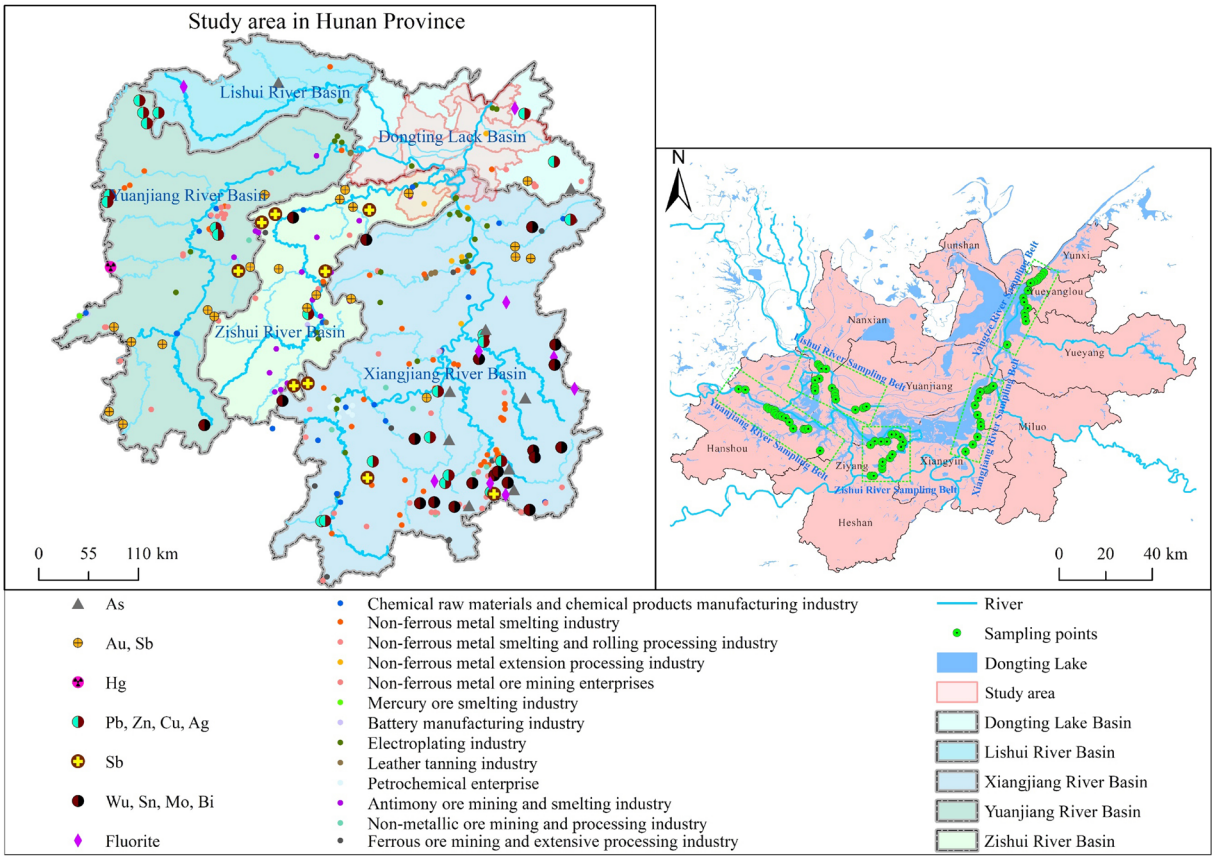

Fig. 1 Location distribution of study area and sampling sites, and distribution of major mineral deposits and HMs-related enterprises in Hunan Province, China

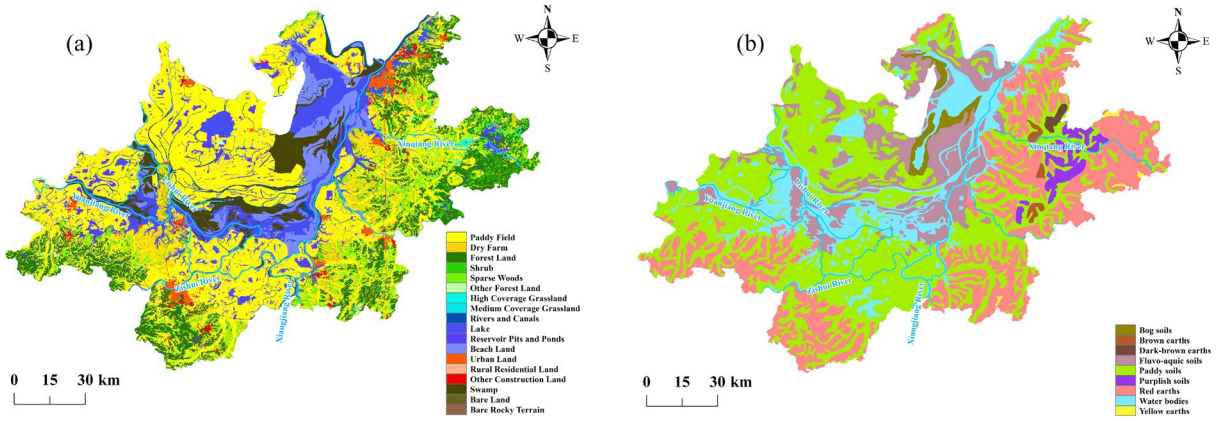

Fig. 2 Spatial distribution map of land use status (a) and soil type (b)

with numerous mining, metallurgy, electroplating, and chemical enterprises (Fig. 1). However, the copious discharge of wastewater from resource extraction and processing has induced significant annual contamination of Dongting Lake with HMs from the Four Rivers. This has taken a severe toll on the lake's ecological environment and the health of surrounding residents. Studies have indicated that the water quality in the Dongting Lake watershed has been polluted to varying degrees, with increasing health risks from HMs [43,44]. Therefore, it is essential to assess the sources and risks of HMs pollution in the surface sediments at the main inlets and outlets of Dongting Lake.

2.2 Sampling and chemical analysis

In light of the geographical location, topography, and geomorphology of Dongting Lake, coupled with the spatial distribution of its principal inlets and outlets as well as water flow direction, 5 sampling belts were set up, and a total of 87 surface sediment samples were collected from July to August 2023 (Fig. 1). According to the Technical Specification for Sediment Environmental Monitoring (HJ 494—2009), five subsamples were retrieved from the 0−20 cm surface sediment layer (within a 100 m × 100 m grid) and then mixed thoroughly to obtain a representative sample (approximately 1−2 kg). Afterward, the samples were immediately sealed in airtight polyethylene bags and transported frozen to the laboratory. The samples were air-dried to remove plant roots, stones, and other impurities, crushed by using an agate mortar, and ground through a nylon sieve. The <2 mm and <0.149 mm fractions were retained for the analysis of pH and HMs (including As, Cd, Co, Cr, Cu, Hg, Mn, Ni, Pb, Sb, Sn, Tl, V and Zn), respectively.

After the samples were digested by the HF−HNO^3−$HClO^4$ system, the concentrations of Tl, Cd, Co, Pb, Cu and Zn were analyzed by inductively coupled plasma mass spectrometry (ICAP QC); the concentrations of Mn, Ni and V were determined by inductively coupled plasma atomic emission spectrometry (ICP-AES); the concentrations of As and Sb were analyzed by atomic fluorescence spectrometry (AFS); the concentration of Hg was determined by cold atomic fluorescence spectrometry (CVAFS); the concentration of Cr was determined by X-ray fluorescence spectrometry (XRF); the concentration of Sn was determined by photoelectric direct reading emission spectrometry (PDS); the pH value was analyzed by ion selective electrode method. To ensure the accuracy of the analytical results, the national first-grade standard substances, GSS-25 and GSS-28, were used as quality control samples. Parallel samples were prepared for each sample, maintaining an analytical error of less than 5%, and the average of the results was used for evaluation. The detection limits of As, Cd, Co, Cr, Cu, Hg, Mn, Ni, Pb, Sb, Sn, Tl, V and Zn were 0.2, 0.021, 0.002, 0.4, 0.6, 0.0005, 0.02, 0.2, 0.5, 0.05, 0.5, 0.003, 0.3 and 1.1 mg/kg, respectively.

2.3 Source apportionment and ecological risk assessment methods

2.3.1 Geo-accumulation index

The geo-accumulation index (I_{geo}) was used to assess the pollution level of HMs in the surface sediments of Dongting Lake [45,46]. The calculation formula of I_{geo} is as follows [47]:

$$I_{\text{geo}}=\log_2\left(\frac{C_j}{1.5B_j}\right) \tag{1}$$

where C_j represents the actual concentration of element j (mg/kg), B_j is the geochemical background value of element j (mg/kg), and the coefficient of 1.5 is usually used to minimize the influence of background value changes that may be caused by soil lithology changes [47]. The corresponding relationship between the I_{geo} value and the pollution level is given in Table 1.

Table 1 Corresponding relationship between contamination level and value for I_{geo}

Contamination level	I_{geo}
Unpolluted	≤0
Lightly polluted	0−1
Lightly to moderately polluted	1−2
Moderately polluted	2−3
Moderately to heavily polluted	3−4
Heavily polluted	4−5
Extremely polluted	>5

2.3.2 Positive matrix factorization

The positive matrix factorization (PMF) model was applied to source apportionment [48]. The core of the PMF model algorithm is to minimize the objective function Q, and its calculation method is as follows [49−51]:

$$X_{ij}=\sum_{k=0}^{p}g_{ik}f_{kj}+e_{ij} \tag{2}$$

$$Q=\sum_{i=1}^{n}\sum_{j=1}^{m}\left[\left(x_{ij}-\sum_{k=1}^{p}g_{ik}f_{kj}\right)\Big/u_{ij}\right] \tag{3}$$

For $c\leq$ MDL,

$$u_{ij}=\frac{5}{6}\text{MDL} \tag{4}$$

Else,

$$u_{ij}=\sqrt{(\text{Ef}_j\cdot C_{ij})^2+\left(\frac{\text{MDL}_j}{2}\right)^2} \tag{5}$$

where i, j and k are the numbers of samples, elements and different sources, respectively; X_{ij} is the concentration of element j in sample i (mg/kg); g_{ik} is the contribution of source k in sample i (mg/kg); f_{kj} is the amount of element j from source k; e_{ij} is the residual; u_{ij} is the uncertainty of element j in sample i; MDL_j is the species-specific method detection limit of element j; Ef_j is the percentage of measurement uncertainty of element j; C_{ij} is the concentration value of element j from sample i, mg/kg.

2.3.3 Source-specific Nemerow integrated risk index

The Nemerow integrated risk index (NIRI) accounts for both toxicity factors and the number of elements. It is a new potential ecological risk assessment method developed by MEN et al [52], based on the Nemerow integrated pollution index (NIPI) and the potential ecological risk index (RI) [53]. The source-specific Nemerow integrated risk index (SI) model quantitatively analyzes the ecological risk of each pollution source by coupling the NIRI with the source apportionment results from the PMF model. The specific calculation formulas are as follows:

$$\text{SI}_{ij}^{k}=\sqrt{\left[(E_{ij\,(\max)}^{k})^2+(E_{ij(\text{avg})}^{k})^2\right]/2} \tag{6}$$

where SI_{ij}^{k} is the integrated ecological risk of pollutant source k for element j in sample i; $E_{ij\,(\max)}^{k}$ and $E_{ij(\text{avg})}^{k}$ denote the maximum and average values, respectively, of the ecological risk for all elements from pollutant source k in sample i.

The calculation formula for E_{ij}^{k} is as follows:

$$E_{ij}^{k}=T_{\text{r}}^{j}\cdot\frac{C_{ij}^{k}}{C_{\text{b}}^{j}} \tag{7}$$

where E_{ij}^{k} represents the ecological risk of the element j from pollutant source k in sample i. T_{r}^{j} is the toxicity response coefficient for HM j. In this study, the toxicity coefficients for As, Cd, Co, Cr, Cu, Hg, Mn, Ni, Pb, Sb, Sn, Tl, V and Zn are set at 10, 30, 5, 2, 5, 40, 1, 5, 5, 10, 1, 40, 2 and 1, respectively [53,54]. C_{b}^{j} uses the background value of element j in Dongting Lake Plain soil [55]. C_{ij}^{k} represents the mass contribution of pollutant source k to element j in sample i, mg/kg.

The calculation formula for C_{ij}^{k} is as follows:

$$C_{ij}^{k}=C_{ij}^{k*}\cdot C_j \tag{8}$$

where C_{ij}^{k*} is the contribution of pollutant source k to element j in sample i; C_{ij} is the measured value of element j in sample i, in mg/kg.

The correspondence between the ecological risk levels and values of SI_{ij}^{k} is shown in Table 2.

Table 2 Relationship between contamination level and value for potential ecological risk index (ER) and source-specific Nemerow integrated risk index (SI)

Contamination level	ER	SI
Low risk	<40	<40
Moderate risk	40−80	40−80
Considerable risk	80−160	80−160
High risk	160−320	160−320
Very high risk	≥320	≥320

3 Results and discussion

3.1 Pollution and spatial distribution characteristics of heavy metals

The descriptive statistical data of the concentrations of 14 HMs in the surface sediment samples of the study area are given in Table 3. The mean concentrations of As, Cd, Co, Cr, Cu, Hg, Mn, Ni, Pb, Sb, Sn, Tl, V, and Zn were 28.64, 2.17, 16.93, 82.33, 37.78, 0.18, 1038.15, 37.50, 52.46, 4.71, 7.66, 0.81, 109.31 and 150.06 mg/kg, respectively. These values were 2.14, 9.44, 1.02, 0.98, 0.82, 2.55, 1.11, 0.90, 1.89, 3.16, 2.47, 0.93, 0.85 and 1.51 times those of the soil background of the Dongting Lake Plain [55], indicating that HMs in the study area, especially Cd, Hg and Sb, were seriously polluted. Additionally, the concentrations of Cd, Hg, Zn, Pb, Sb and Sn at over 70% of the sample points exceeded the background values, suggesting that these elements may pose significant ecological risks in the study area. Kurtosis and skewness are mainly used to measure the distribution state of data. Previous studies have shown that the concentration distribution of soil elements developed under the natural soil-forming state should follow the normal distribution [56]. As can be seen from Table 3 that except for Co, Cu, Ni, Tl, and V, the skewness values of the remaining elements are all greater than 1, belonging to positive skewness. Moreover, the kurtosis values of these elements are relatively high, indicating that the distribution of the concentrations of these elements is subject to different degrees of external interference. Meanwhile, As, Cd, Hg, Pb, Sb, Sn and Zn show a high degree of spatial variation (CV>50%), and especially the variation coefficients of Cd and Sb exceed 100%, reaching 124.69% and 122.71%, respectively. The above results imply that elements such as As, Cd, Hg, Pb, Sb, Sn and Zn within the study area are likely to be influenced by human activities. Among them, Cd and Sb are particularly affected, presumably on account of point source pollution.

To assess the impact of the anthropogenic activities on the HMs concentrations in the surface sediments of the study area, the I_{geo} was calculated and analyzed (Fig. 3). The mean I_{geo} values of heavy metals in the study area are ordered as follows:

Table 3 Descriptive statistics of HMs concentrations in surface sediments of Dongting Lake

Element	Concentration/(mg kg^{-1})					CV/%	Skewness	Kurtosis	BV/ (mg kg^{-1})	Increasing times
	Min.	Max.	Mean	Median	SD					
As	7.32	212.00	28.64	19.40	28.46	99.35	3.69	19.79	13.41	2.14
Cd	0.12	12.20	2.17	0.92	2.71	124.69	2.04	3.69	0.23	9.44
Co	9.65	24.90	16.93	17.00	3.35	19.80	−0.08	−0.28	16.58	1.02
Cr	47.90	136.00	82.33	83.20	15.71	19.09	0.50	1.31	83.92	0.98
Cu	19.60	79.20	37.78	35.55	12.67	33.53	0.94	0.78	45.86	0.82
Hg	0.04	0.92	0.18	0.14	0.13	75.46	3.44	15.90	0.07	2.55
Mn	356.00	3155.00	1038.15	904.50	477.24	45.97	1.79	4.14	938.00	1.11
Ni	21.10	58.00	37.50	37.05	7.72	20.60	0.11	−0.36	41.80	0.90
Pb	23.90	162.00	52.46	37.20	29.23	55.72	1.48	2.18	27.75	1.89
Sb	0.60	34.00	4.71	3.02	5.78	122.71	3.21	11.81	1.49	3.16
Sn	2.12	40.20	7.66	4.50	6.99	91.23	2.09	5.19	3.10	2.47
Tl	0.44	1.21	0.81	0.79	0.17	20.93	0.30	−0.66	0.88	0.93
V	63.60	152.00	109.31	108.00	18.07	16.53	−0.13	0.10	128.00	0.85
Zn	69.00	633.00	150.06	121.00	85.76	57.15	2.94	12.19	99.67	1.51

SD: Standard deviation; CV: Coefficient variation; BV: Background values of HMs in soil from Dongting plain [55]

Cd (1.90) > Hg (0.54) > Sb (0.46) > Sn (0.3) > Pb (0.16) > As (0.09) > Zn (−0.14) > Mn (−0.54) > Co (−0.58) > Cr (−0.63) > Tl (−0.73) > Ni (−0.77) > V (−0.83) > Cu (−0.94). Among them, Cd has the highest pollution level, with a mean I_{geo} value of 1.90. The overall pollution level of Cd is classified as lightly to moderately polluted, with 34.12% of its sample points falling into moderate or higher pollution levels, and 11.76% reaching heavily polluted or worse levels; The average I_{geo} values of Hg, Sb, Sn, Pb and As are at the lightly polluted level, and the overall pollution situation is relatively light, with the proportions of samples that have not reached the moderately polluted level being 96.47%, 88.24%, 91.76%, 100.00% and 96.47%, respectively; The average I_{geo} values of the remaining elements are below 0, indicating an unpolluted level. Among these, Co, Cr, Cu, Ni, Tl and V exhibit the lowest pollution levels, with almost all samples showing no pollution, whereas Zn and Mn are slightly polluted. Comprehensive analysis shows that the pollution levels of Co, Cr, Cu, Ni, Tl and V are relatively low and may be less affected by human activities. Overall, Cd is the most polluted, followed by Hg and Sb, which exhibit heavy concentration characteristics, indicating that Cd, Hg and Sb are seriously affected by human sources. The results show that despite various environmental control measures, some HMs in the Dongting Lake area still pose pollution risks due to anthropogenic activities.

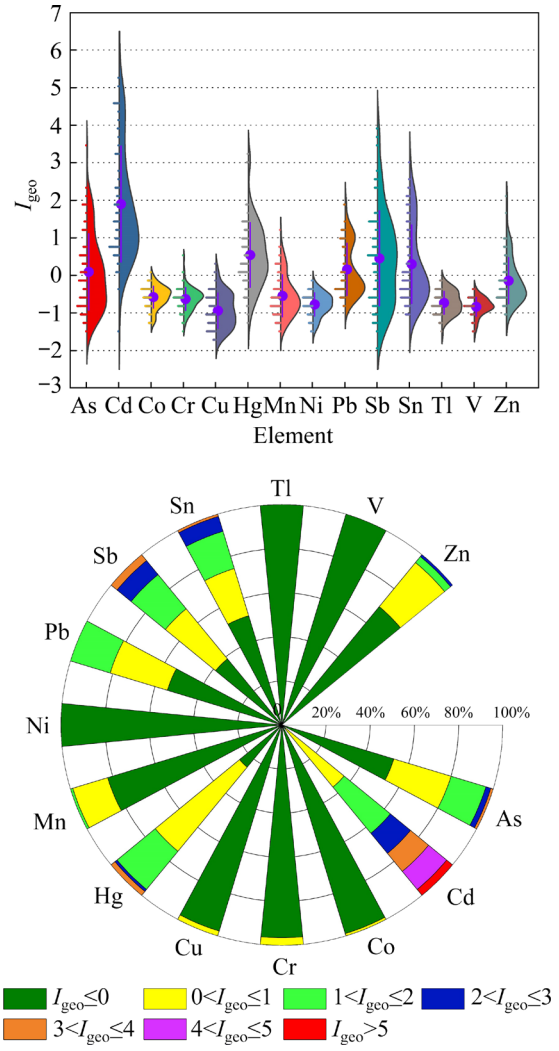

Fig. 3 Geo-accumulation index (I_{geo}) value and grade statistical map of individual HM in surface sediments

Information on the spatial distribution of HMs aids in thoroughly exploring the extent of surface sediment contamination in the study area and analyzing potential sources of contamination. The spatial distribution characteristics of 14 HMs in the surface sediments around Dongting Lake are illustrated in Fig. 4. Due to the uniqueness of the current land use, soil types, mineral resources and industrial distribution within the Four Rivers watersheds, the spatial distribution characteristics of the concentrations of 14 HMs exhibit distinct variations. The spatial distributions of As, Cd, Mn, Pb, Sn, Tl and Zn exhibit similar patterns, with elevated concentrations primarily in the XR and Yangtze River sediments (Figs. 4(a, b, g, i, k, l, n)). These HMs mainly originate from industrial manufacturing, chemical production as well as the mining of non-ferrous and ferrous metal minerals. As the core production base for major metal minerals in Hunan Province, the XR watershed hosts numerous enterprises involved in the mining, beneficiation, and processing of non-ferrous metals, ferrous metals, and non-metallic minerals, and has developed various HM-related enterprises, such as those in the chemical raw materials and chemical products manufacturing industry, electroplating industry, leather tanning and processing industry, and petrochemical enterprises. Meanwhile, the Yangtze River outlet, as the convergence point of the water flow of Dongting Lake, not only receives the wastewater discharged by the mining industry, paper mills, chemical enterprises, and petro-chemical enterprises but also experiences the process that the inflow water and precipitation enhance the flocculation of HMs and precipitation of suspended particles. The concentrations of Co, Cr, Cu, Ni and V are elevated in the LR sediments,

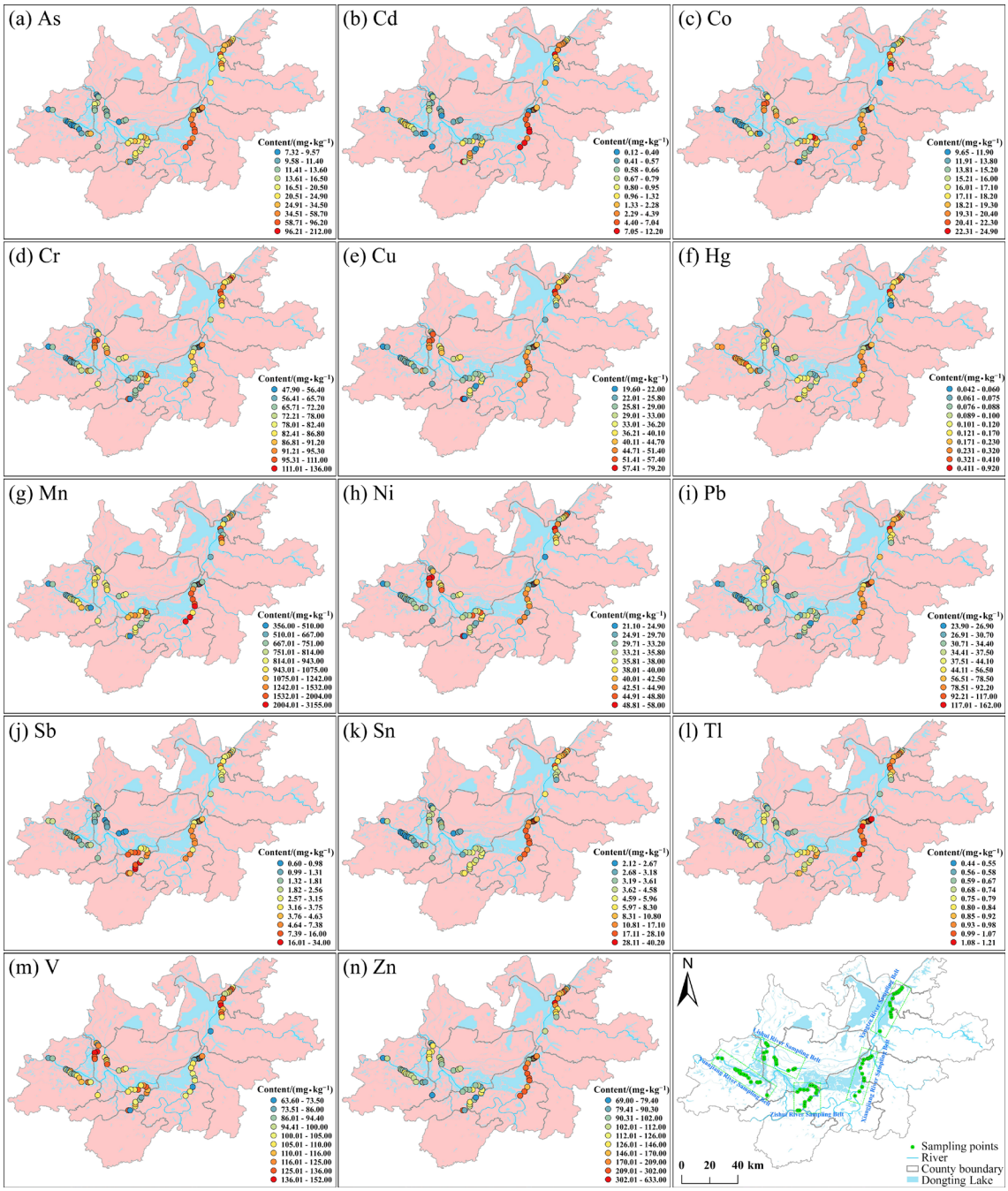

Fig. 4 Spatial distribution of HMs in surface sediments of Dongting Lake

with a few high value points in the XR and Yangtze River sediments, while concentrations are lower in the YR and ZR sediments (Figs. 4(c, d, e, h, m)). Previous studies have shown that Co, Cr, Cu, Ni and V mainly originate from natural erosion, non-point agricultural pollution and aquaculture [1,19]. The LR watershed is abundant in forest and land resources. It features well-developed tourism and agriculture sectors, a thriving aquaculture industry at its estuary, along with substantial reserves of mineral resources, including coal, cuprum and manganese. The spatial distribution of Hg differs from that of other HMs, with high-value points mainly located in YR and XR sediments. The YR spans the Tongren−Fenghuang mercury ore belt in Hunan Province and Guizhou Province, the latter of which is known as “the mercury town of China”. Guizhou Province has the largest reserve of Hg resources in Asia and ranks third globally in terms of mercury production. Therefore, the background

level of Hg in the YR sediments is high [57,58] (Fig. 4(f)). The high-value points of Sb are concentrated in the ZR sediments, with additional high-value points in the LR and XR sediments (Fig. 4(j)). The enrichment of Sb stems from the discharge of antimony-containing industrial wastewater and waste residues from antimony-containing rock or coal mining. The most concentrated and important area for the distribution, mining and smelting of antimony ores in Hunan Province is the ZR watershed. The XR watershed is relatively rich in mineral resources such as coal and antimony, while the LR watershed also possesses a certain quantity of coal reserves.

3.2 Source apportionment of HMs

3.2.1 Correlation analysis of HMs

Pearson correlation analysis was conducted to explore the homology of HMs in the surface sediments of Dongting Lake (Fig. 5) [10,59]. Strong and significant positive correlation was found among As, Cd and Mn (r>0.74). Correlation among As, Pb, Sn and Tl was also significantly positive (r>0.48), especially for Pb and Sn, with r-value reaching 0.93. The correlation coefficients among Co, Cr, Ni and V were relatively large (r>0.57), and each pair showed an extremely significantly positive correlation (p≤0.001). The good correlations within these three groups of elements indicate that the elements within each group may have the same source [60]. The correlation between Hg and Sb and other elements is weak, indicating that they may come from different pollution sources. Comprehensive analysis reveals that the sources of HMs in the study area are relatively complex, and more in-depth and detailed analysis is required.

3.2.2 Sources apportionment by PMF

Based on the EPA PMF5.0 software, we conducted the pollution sources analysis of HMs in surface sediments, identified the potential sources of each HM in the study area, and quantified the contribution ratios of various pollution sources to each HM. During the quantitative source analysis process of PMF, the signal-to-noise ratios of 14 HMs were all greater than 4.8 and were set as “Strong”. Through multiple adjustments of the number of factors, it was found that the model was the most stable when the number of factors was 5. At this time, Q_{rob}/Q_{exp} was the minimum, and the best fitting effect was achieved between the measured concentration value and the predicted value of the model. The residual values of the vast majority of samples fell between −3 and 3 and followed the normal distribution [48,61]. The results of the fitting coefficient (R^2) of each element

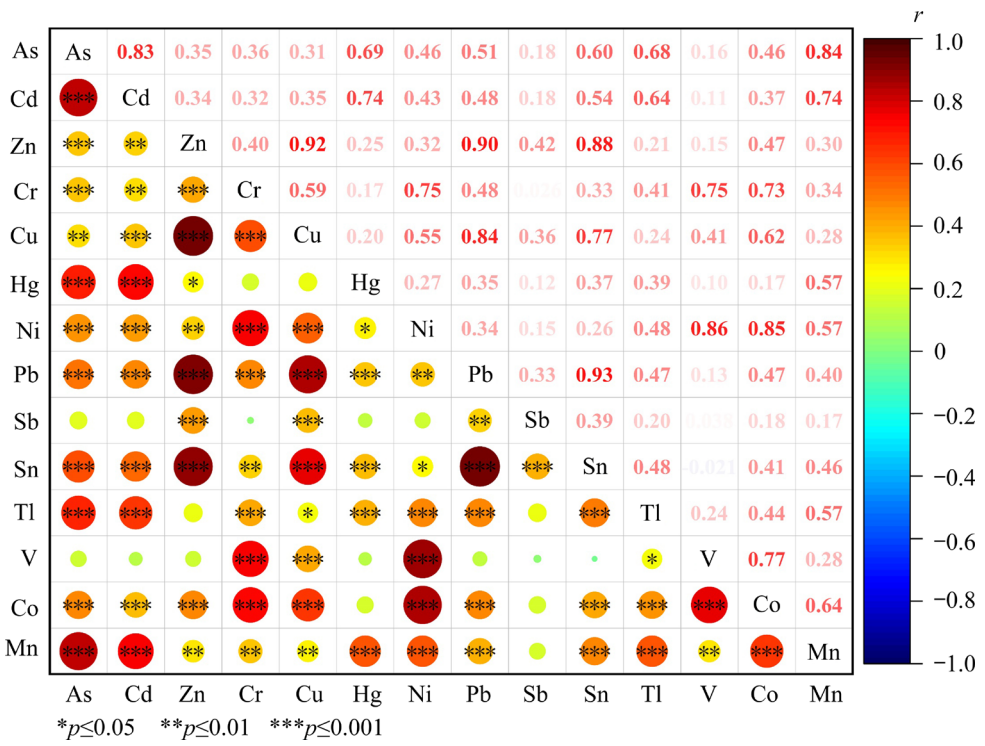

Fig. 5 Correlation coefficient heat map for HM concentrations in surface sediments

show that except for the R^2 of elements Cr, Cu, Hg, Pb and Co being 0.71, 0.8, 0.76, 0.83 and 0.81 respectively, the R^2 values of the remaining elements are all greater than 0.91. Therefore, the number of factors selected by this calculation scheme is reasonable and can better explain the information contained in the original data source. Figure 6 presents the factor distribution and corresponding contributions of each HM under the analysis of the PMF model. In this study, the PMF model parsed out a total of five source factors. Additionally, the Getis-Ord Gi* analysis in ArcGIS was employed to detect the positions where the high-value or low-value elements of each factor clustered in space, and the inverse distance weighting method was applied to generating the pollution source distribution map of the study area (Fig. 7). Figure 7 not only provides intuitive information on the influence of each pollution source, but also makes important supplements and confirmations to the PMF analysis results [50,62].

Factor 1 (F1) accounted for 17.99% of the factor contribution, among which Hg (57.67%) dominated. As given in Table 3, the coefficient of variation for Hg was 75.46%, which was a strong variation level, suggesting a significant influence by anthropogenic factors. As can be seen from Fig. 7(a), samples with markedly low points for F1 were primarily clustered in the ZR and XR sediments, whereas samples with conspicuously high points for F1 were mainly distributed in the YR watershed, where numerous mercury deposits were concentrated. This is consistent with the results depicted in the spatial distribution map generated via inverse-distance interpolation. Field surveys and data collection show that the upper

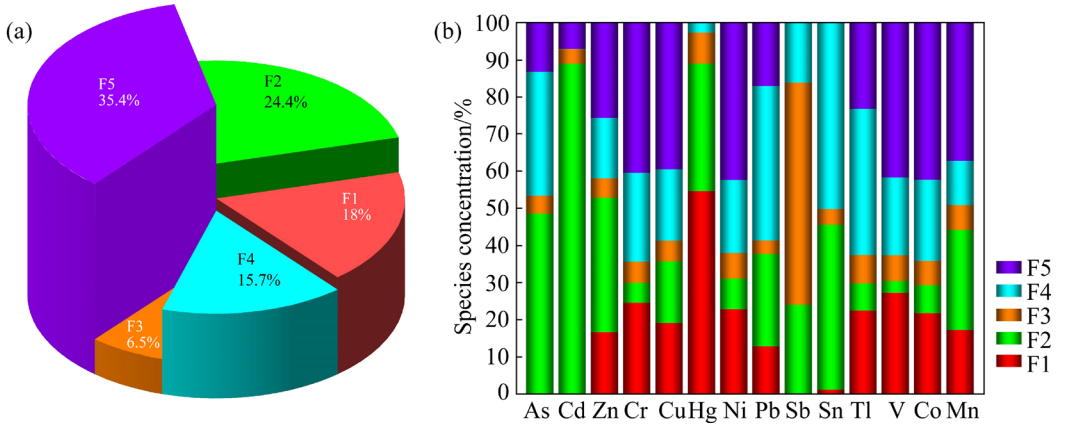

Fig. 6 Source apportionment of HMs in surface sediments on Dongting Lake: (a) Percent factor contribution based on PMF model; (b) Species contribution of 5 factors for HMs based on PMF model

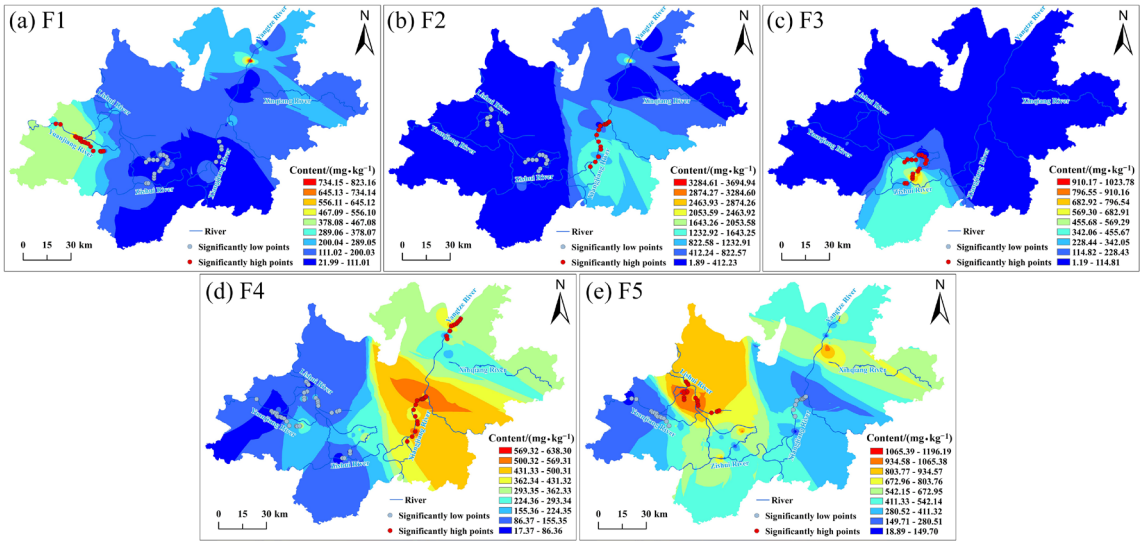

Fig. 7 Overlay map for spatial distribution of each factor by PMF model and spatial distribution of high-low value

reaches and left tributaries of the YR river system flow through the largest mercury ore belt in China, namely the Hunan−Guizhou Mercury Ore Belt. The average concentration of Hg in the surface sediments at the YR sampling belt was the highest, which was mainly related to the mercury mining activities represented by the Wanshan Mercury Mine, Tongren Mercury Mine, Xinhuang Mercury Mine and Fenghuang Chatian Mercury Mine in the middle and upper reaches of the YR river system, and also related to the relatively high background concentration of Hg in the YR sediments [58]. Multiple studies have demonstrated that Hg possesses high volatility and can easily migrate and diffuse over long distances with the atmosphere at elevated temperatures [20,63]. In addition, F1 also had a considerable contribution to Tl (22.49%). Previous studies have shown that Tl also has a certain volatility [64], which indirectly proves the characteristics of the atmospheric migration source of F1. Therefore, F1 may be related to mercury ore smelting or atmospheric migration.

Factor 2 (F2), which contributed 24.44%, had an intermediate species contribution for Cd (88.94%), As (48.55%) and Mn (26.91%), followed by Zn (36.23%), Hg (34.32%) and Sn (44.45%). The significant high points of F2 were clustered in the XR watershed, where urban agglomerations and other construction lands were densely distributed (Fig. 7(b)). The results of its inverse distance weighted interpolation were also consistent with the results of the Getis-Ord Gi* point analysis, and obvious point sources were shown in the high-value areas. The spatial distributions of As, Cd, Mn, Sn and Zn were similar, with high-concentration points mainly located in the XR and Yangtze River sediments (Fig. 4). According to the land use status map (Fig. 2(a)), there was a significant amount of construction land around the XR and Yangtze sediments. The Yangtze River sampling belt was located in Yueyang City. During the historical process of urban transformation, various industries related to HMs have emerged, including mining, paper mills, chemical and petrochemical enterprises, mechanical industries, as well as hardware processing and electroplating enterprises. The HM-containing wastewater discharged by these enterprises was an important source of HMs accumulation in surface sediments. In addition, the incoming water of the Yangtze River enhanced the flocculation and precipitation of suspended particles [10]. The XR watershed was the most developed and urbanized area in Hunan Province. Changsha, Zhuzhou, Xiangtan and Chenzhou along the XR river were the concentrated areas of heavy chemical industries such as nonferrous metals, chemicals, steel, mines and smelting in Hunan Province [35,38,65]. The XR was the largest river and an important sewage-receiving water body in Hunan Province [66]. According to the "Environmental Quality Report of Hunan Province", the industrial sewage and domestic sewage received by the XR each year were 5.7×10^9 t and 1.055×10^{10} t, accounting for 56.94% and 69.40% of the industrial sewage and domestic sewage of Hunan province, respectively. Zhuzhou Smelting Group, Shuikoushan Group, Salt Factory Chemical Group, Hunan Haili Chemical Group, Xiangtan Electrochemical Group, Hualing Iron and Steel Enterprise, as well as many small smelting workshops, chemical enterprises and printing factories were located along the XR river [10]. According to the environmental protection bureau of the Hunan province, the emission loads of Hg, Pb, Cd and As from XR were accounted for 54.5%, 37.0%, 6.0% and 14.1% in the national emissions of year 2007, respectively. Hence, F2 mainly came from urban domestic sewage and industrial sewage discharge.

The contribution rate of Factor 3 (F3) was 6.50%, mainly related to Sb (59.83%). The spatial distribution maps of HMs (Fig. 4) revealed that the enrichment of Sb in the Four Rivers watersheds was markedly different from that of other HMs. The highest average concentration of Sb was observed in the ZR sediments with 11.48 mg/kg, which was 7.70 times that of the soil background value of 1.49 mg/kg in the Dongting Lake Plain (Table 3). The XR sediments ranked second, with an average concentration of 5.29 mg/kg, or 3.55 times the background value. In comparison, the average concentrations in the YR and LR sediments were relatively low. The significant low points of F3 were predominantly concentrated in the LR sediments, while a smaller proportion was distributed across the YR sediments, and the significant high points were predominantly aggregated in the ZR sediments (Fig. 7(c)). This enrichment disparity corresponds to the notable geological background difference observed in the

Four Rivers watersheds and is also significantly related to the types of metal deposits distributed across the Four Rivers watersheds [13]. The antimony ore reserves in the ZR watershed constituted 80.00% of the world's total antimony reserves. Additionally, the watershed exhibited extensive enrichment of ferrous metals, such as iron and manganese, as well as non-ferrous metal deposits, with relatively simple metallogenic elements. It was a principal antimony ore resource distribution area in Hunan Province, including notable deposits such as Xikuangshan, Zhazixi, and Banxi [26]. Regions such as Loudi, Shaoyang, and Yiyang, situated within the ZR watershed, served as the principal centers for antimony mining and smelting in Hunan Province [34,39]. Zhang et al [40] demonstrated that antimony smelters were extensively distributed in the middle reaches of the ZR watershed, where Sb pollution was most severe due to the historical development and expansion of antimony mining and smelting enterprises. For instance, several large antimony deposits are located in the ZR watershed. Its tributaries, such as the Lianxiche and Qingfenghe rivers, have been heavily polluted, which has an adverse impact on the water quality of the main stream of the ZR river. As mentioned above, we believe that F3 represents the source of antimony mining and smelting.

Factor 4 (F4), with factor contribution of 15.72%, was mainly loaded on Sn (50.15%), Pb (41.60%), Tl (39.36%), As (33.37%) and Zn (16.24%). The inverse distance weighted interpolation and Getis-Ord Gi* analysis showed that the high-value area of F4 was concentrated in the XR and Yangtze River sediments (Fig. 7(d)), which was consistent with the spatial distribution characteristics of Sn, Pb, Tl, As and Zn (Fig. 4). In the XR and Yangtze River watersheds, numerous mining and smelting enterprises for non-ferrous and ferrous metal minerals have established the core production base for major metal minerals in Hunan Province [38,67,68]. For example, the Changning Shuikoushan Lead−Zinc Polymetallic Mine, Guiyang Qinglan Tin−Lead−Zinc Polymetallic Mine, Guiyang Baoshan Lead−Zinc Polymetallic Mine, Yizhang Yaogangxian Tungsten Polymetallic Mine, and Guiyang Huangshaping Lead−Zinc Polymetallic Mine were located in the XR watershed. The Taolin Lead−Zinc Polymetallic Mine was located in the Xinqiang watershed, among others. In addition, Yueyang City served as the main port for mining activities in Hunan Province, with 11 large deposits, 16 medium-sized deposits and 27 small deposits [10]. Simultaneously, four important smelting sites were located in the XR watershed: Chenzhou Sanshiliuwan, Hengyang Shuikoushan, Zhuzhou Xiawangan and Xiangtan Zhubugang [69]. In non-ferrous metallurgy, especially lead−zinc smelting, the concentrations of Sn, Pb, Tl, As and Zn in the wastewater are significantly higher than those in the wastewater of other industries [70]. Owing to the limited environmental awareness among the ancients, vast quantities of slags were piled up in the open air. This led to a significant quantity of HMs being leached out, which were then discharged into Dongting Lake via surface runoff. In the estuary area, the decrease in flow velocity triggered the precipitation of HMs within the sediments, resulting in significant accumulation and release of Sn, Pb, Tl, As and Zn. Therefore, F4 was identified as an industrial source of non-ferrous metal smelting and extended processing.

Factor 5 (F5), which contributed 35.35%, was mainly characterized by Co (42.30%), Cr (40.47%), Cu (39.50%), Ni (42.40%), V (41.70%), and Mn (37.18%), and also had a considerable contribution value to Zn (25.64%) and Tl (23.20%). According to Table 3, the average concentrations of Co, Cr, Ni, Tl and V were relatively low, all approaching the soil background value of the Dongting Lake Plain [55], and the coefficient of variation was small, indicating that these HMs were less influenced by human activities. Meanwhile, most samples of these HMs were not polluted. The I_{geo} index showed that proportion of samples with $I_{geo} \leq 0$ for Co, Cr, Cu, Ni, Tl and V exceeded 96.47%. Previous studies have shown that Co, Cr, Ni and V mainly originate from soil parent materials [26,71−73]. Furthermore, by comparing the spatial distribution of the PMF model analysis factors with the high-low value point overlay map (Fig. 7) of F5 and other pollution source factors, we found that the primary feature of the F5 value was the concentration of significant high points and high-value areas in the LR sediments. The LR watershed is agriculture advanced, encompassing a vast area of arable land (approximately 3.18×10^9 m^2) and numerous fisheries and farms, where substantial amounts of pesticides, fertilizers, and feed are applied annually

to optimizing yields. Multiple studies had shown that pesticides, fertilizers, feed and animal manure contain a large amount of elements of Co, Cu, Mn, Zn, C, Ni, Tl and V [10,36,67,73]. Hence, F5 represented a mixed source mainly based on natural and agricultural sources.

From the above analyses, it could be seen that As, Zn, Hg, Sn, Tl and Mn dominate among multiple factors (As (F2 (48.55%) + F4 (33.37%)), Zn (F2 (36.23%) + F4 (16.24%) + F5 (25.64%)), Hg (F1 (54.67%) + F2 (34.32%)), Sn (F2 (44.45%) + F4 (50.15%)), Tl (F1 (22.49%) + F4 (39.36%) + F5 (23.20%)), Mn (F2 (26.91%) + F5 (37.18%))), indicating that As, Zn, Hg, Sn, Tl and Mn in the surface sediments of Dongting Lake were jointly affected by multiple sources.

3.3 Source-specific ecological risk assessment

The evaluation results of the single ecological risk index (ER) of HMs in the surface sediments of Dongting Lake (Fig. 8(a)) showed that the ecological risk values of Cd, Hg and Sb in the samples were relatively dispersed. Among them, the average ER value of Cd was the highest, at 281.45, placing it in the high-risk category (160−320). Moreover, the ER values of some samples even reached the very high-risk level, indicating that Cd in the study area posed a strong ecological risk. Secondly, the average ER value of Hg was 101.14, placing it at the considerable risk level (80−160). Notably, the ER values of some samples exceeded 160, ascending to the high-risk level, which indicated a relatively strong ecological risk associated with Hg in the study area. The average ER values of As, Zn, Cr, Cu, Ni, Pb, Sb, Sn, Tl, V, Co and Mn were 21.30, 1.71, 1.97, 4.32, 4.49, 10.06, 33.33, 2.71, 36.94, 1.71, 5.14 and 1.11, respectively, categorizing them within the low risk level. Among them, some samples of As, Sb, Pb and Tl were at the moderate or considerable risk level, and there was a certain ecological risk. The ER values of all samples of the remaining HMs were less than 40, and the ecological risk was extremely low.

The evaluation results of the SSNIRI in the study area (Fig. 8(b)) indicated that among the 14 HMs, Cd, Hg, Tl, Sb and As contributed significantly to the integrated ecological risk, indicating that these HMs, especially Cd and Hg, should be prioritized for monitoring to mitigate further environmental pollution in the study area. The contributions of the five pollution sources to the integrated ecological risk of the surface soil of Dongting Lake were ranked as follows: F2 (68.63%) > F1 (15.17%) > F3 (6.09%) > F5 (5.79%) > F4 (4.32%). From this, it could be inferred that F2 and F1 imposed a relatively high ecological risk to Dongting Lake. However, the PMF analysis results demonstrated that F2 and F1 accounted for only 24.4% and 18.0%, respectively, of the sources of HMs in the study area. In contrast, their contributions to the NIRI of the study area were 68.63% and 15.17%, respectively, which were significantly higher than those of other pollution sources. This may be attributed to the relatively low background values of Cd, As and Hg, as well as their high toxicity coefficients in the study area [74].

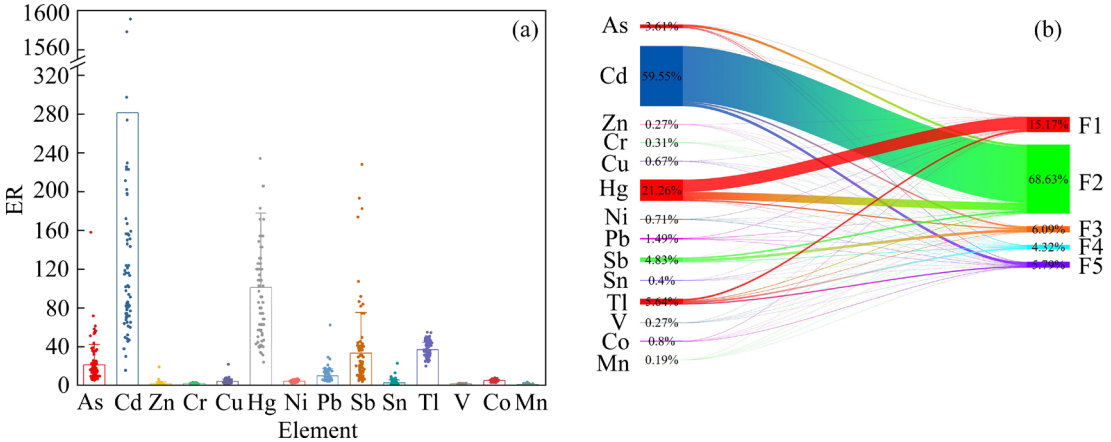

Fig. 8 Ecological risk assessment of HMs in surface sediments of Dongting Lake: (a) Distribution of single ecological risk index (ER) at each sampling point; (b) Contributions of each factor by PMF model and each HM to source-specific Nemerow integrated risk index (SI)

The above results indicated that the contributions of pollution sources to the SI did not necessarily correspond to their contributions to HMs; the urban domestic sewage and industrial wastewater discharge source (F2), as well as the mixed source of mercury ore smelting and atmospheric migration (F1) in the Dongting Lake area were priority control pollution sources; Cd, Hg, Tl, Sb and As were priority control HMs in the Dongting Lake area.

4 Conclusions

(1) Co, Cr, Cu, Ni and V in Dongting Lake are less polluted and less affected by anthropogenic activities; As, Cd, Hg, Pb, Sb, Sn and Zn are polluted to a certain extent, with Cd, Hg and Sb being the most seriously polluted.

(2) The spatial distribution characteristics of the 14 HMs in surface sediments exhibited significant variations, with distinct concentration patterns across different watersheds. High concentrations of As, Cd, Mn, Pb, Sn, Tl and Zn were located in the Xiangjiang and Yangtze rivers sediments; high concentrations of Co, Cr, Cu, Ni and V were found primarily in the Lishui river sediments; the high concentrations of Hg and Sb were mainly located in the Yuanjiang and Zishui rivers sediments, respectively.

(3) The accumulation of HMs was primarily influenced by 5 pollution sources, with the contributions and key loading elements of each source being detailed as follows: the mixed source of mercury ore smelting and atmospheric migration (17.99%), accounted for 57.75% of Hg contamination; urban domestic sewage and industrial sewage source (24.44%), was mainly characterized by Cd (88.92%), As (48.55%), Zn (36.23%), and Hg (34.37%); antimony mining and smelting source (6.50%), was responsible for 59.83% of Sb pollution; non-ferrous metal smelting and ductile processing industrial sources (15.72%), led to 50.15% of Sn, 41.60% of Pb, 39.36% of Tl and 33.37% of As pollution; mixed natural and agricultural sources (35.35%), were characterized primarily by Cr (40.55%), Cu (39.58%), Ni (42.46%), V (41.47%), and Co (42.33%). The sources of elements such as As, Zn, Hg, Sn, Tl and Mn in the surface sediments of Dongting Lake were not singular but resulted from the combined influence of multiple pollution sources.

(4) Some samples of Cd, Hg, As, Sb, Pb and Tl in the study area posed certain ecological risks, while the ecological risk levels of the remaining elements were very low. Source-specific ecological risk assessment of Dongting Lake indicated that urban domestic sewage and industrial sewage discharge source, as well as the mixed source of mercury ore smelting and atmospheric migration, had the greatest contribution to the ecological risk of Dongting Lake and was the priority control pollution source; Cd, Hg, Tl, Sb and As, especially Cd and Hg, were the priority control pollution elements.

CRediT authorship contribution statement

Yao ZHOU: Conceptualization, Methodology, Software, Investigation, Data curation, Validation, Formal analysis, Writing − Original draft, Writing − Review & editing, Visualization; **Yong-sheng CHENG**: Conceptualization, Funding acquisition, Investigation, Supervision, Writing − Review & editing.

Declaration of competing interest

The authors declare that they have no known competing financial interests or personal relationships that could have appeared to influence the work reported in this paper.

Acknowledgments

This work was financially supported by the Key Research and Development Program of Hunan Province, China (No. 2023SK2006), the Natural Science Foundation of Hunan Province, China (No. 2023JJ50057), the Science and Technology Plan Project of Geological Bureau of Hunan Province, China (No. HNGSTP202411), the Open Project of Key Laboratory of the Ministry of Natural Resources, China (No. BL202105), and the Natural Science Foundation of Changsha City, China (No. kq2202090).

References

[1] XIA Fang, ZHAO Ze-fang, NIU Xiang, WANG Zhen-feng. Integrated pollution analysis, pollution area identification and source apportionment of heavy metal contamination in agricultural soil [J]. Journal of Hazardous Materials, 2024, 465: 133215. DOI: 10.1016/j.jhazmat.2023.133215

[2] LIU Zhi-lou, CHEN Zhi-kang, SUN Fu-ze, ZHANG Zhi-heng, YAN kang, ZHONG Shui-ping, LIU Hui, WANG Rui-xiang, LI Jia-yuan, XU Zhi-feng. Separation of halogens and recovery of heavy metals from secondary copper smelting dust [J]. Transactions of Nonferrous Metals Society

of China, 2024, 34: 2686−2701. DOI: 10.1016/S1003-6326(24)66569-6

[3] ESMAEILZADEH M, TAVAKOL M, MOHSENI F, MAHMOUDI M, NGUYEN U P, FATTAHI M. Biomarkers for monitoring heavy metal pollution in the Anzali Wetland [J]. Marine Pollution Bulletin, 2023, 196: 115599. DOI: 10.1016/j.marpolbul.2023.115599

[4] LIU Bing-xiang, LUO Jun, JIANG Shou, WANG Yan, LI Yu-cheng, ZHANG Xue-sheng, ZHOU Shao-qi. Geochemical fractionation, bioavailability, and potential risk of heavy metals in sediments of the largest influent river into Chaohu Lake, China [J]. Environmental Pollution, 2021, 290: 118018. DOI: 10.1016/j.envpol.2021.118018

[5] SPRAGUE D D, VERMAIRE J C. Legacy arsenic pollution of lakes near cobalt, Ontario, Canada: Arsenic in lake water and sediment remains elevated nearly a century after mining activity has ceased [J]. Water, Air, & Soil Pollution, 2018, 229(3): 87. DOI: 10.1007/s11270-018-3741-1

[6] OYEWUMI O, FELDMAN J, GOURLEY J R. Evaluating stream sediment chemistry within an agricultural catchment of Lebanon, Northeastern USA [J]. Environmental Monitoring and Assessment, 2017, 189: 141. DOI:10.1007/s10661-017-5856-z

[7] ZHOU yao, CHENG Yong-sheng, WANG Dan-pin, ZHANG Ze-wen, ZENG De-xing, LI Xiang-yang, MAO Chun-wang. Hyperspectral inversion of soil arsenic content in polymetallic mining areas based on optimized spectral index combined with PLSR [J]. The Chinese Journal of Nonferrous Metals, 2024, 34(2): 653−667. (in Chinese). DOI: 10.11817/j.ysxb.1004.0609.2023-44331

[8] ESMAEILZADEH M, MEHDINIA A. Origin and comprehensive risk assessment of heavy metals in surface sediments along the Caspian Sea [J]. Marine Pollution Bulletin, 2024, 205: 116587. DOI: 10.1016/j.marpolbul.2024.116587

[9] KACHOUEIYAN F, KARBASSI A, NASRABADI T, RASHIDIYAN M, DE-LA-TORRE G E. Speciation characteristics, ecological risk assessment, and source apportionment of heavy metals in the surface sediments of the Gomishan wetland [J]. Marine pollution bulletin, 2024, 198: 115835. DOI: 10.1016/j.marpolbul.2023.115835

[10] LI Fei, HUANG Jin-hui, ZENG Guang-ming, YUAN Xing-zhong, LI Xiao-dong, LIANG Jie, WANG Xiao-yu, TANG Xiao-jiao, BAI Bing. Spatial risk assessment and sources identification of heavy metals in surface sediments from the Dongting Lake, Middle China [J]. Journal of Geochemical Exploration, 2013, 132: 75−83. DOI: 10.1016/j.gexplo.2013.05.007

[11] BAI Jun-hong, CUI Bao-shan, CHEN Bin, ZHANG Ke-jiang, DENG Wei, GAO Hai-feng, XIAO Rong. Spatial distribution and ecological risk assessment of heavy metals in surface sediments from a typical plateau lake wetland, China [J]. Ecological Modelling, 2011, 222(2): 301−306. DOI: 10.1016/j.ecolmodel.2009.12.002

[12] SURESH G, SUTHARSAN P, RAMASAMY V, VENKATACHALAPATHY R. Assessment of spatial distribution and potential ecological risk of the heavy metals in relation to granulometric contents of Veeranam lake sediments, India [J]. Ecotoxicology and Environmental Safety, 2012, 84: 117−124. DOI: 10.1016/j.ecoenv.2012.06.027

[13] FANG Xiao-hong, PENG Bo, ZHANG Kun, ZENG Deng-zhi, KUANG Xiao-liang, WU Bei-juan, TU Xiang-lin, SONG Zhao-liang, XIAO Yao, YANG Zi-xuan, XIE Wei-cheng, BAO Zhi-cheng, TAN Chang-yin, WANG Xin, WAN Dajuan. Geochemistry of major and trace elements in sediments from inlets of the Xiangjiang and Yuanjiang River to Dongting Lake, China [J]. Environmental Earth Sciences, 2018, 77(2): 16.1−16.16. DOI:10.1007/s126 65-017-7193-5

[14] HE Zhen-li, YANG Xiao-e, STOFFELLA P J. Trace elements in agroecosystems and impacts on the environment [J]. Journal of Trace Elements in Medicine and Biology, 2005, 19(2/3): 125−140. DOI: 10.1016/j.jtemb.2005.02.010

[15] ZAYNAB M, AL YAHYAI R, AMEEN A, SHARIF Y, ALI L, FATIMA M, KHAN K A, LI Shuang-fei. Health and environmental effects of heavy metals [J]. Journal of King Saud University−Science, 2022, 34(1): 101653. DOI: 10.1016/j.jksus.2021.101653

[16] ZHANG Hai-li, ZHAO Peng, GAO Wen-yan, XIAO Bao-hua, YANG Xue-feng, SONG Lei, FENG Xiang, GUO Lin, LU Yong-ping, LI Hai-feng, SUN Jing. Contaminant transport modelling of heavy metal pollutants in soil and groundwater: An example at a non-ferrous smelter site [J]. Journal of Central South University, 2024, 31(4): 1092−1106. DOI: 10.1007/s11771-024-5639-y

[17] BRIFFA J, SINAGRA E, BLUNDELL R. Heavy metal pollution in the environment and their toxicological effects on humans [J]. Heliyon, 2020, 6(9): e04691. DOI: 10.1016/j.heliyon. 2020.e04691

[18] CUI Yong-bo, BAI Li, LI Chun-hui, HE Zi-jian, LIU Xin-ru. Assessment of heavy metal contamination levels and health risks in environmental media in the northeast region [J]. Sustainable Cities and Society, 2022, 80: 103796. DOI:10.1016/j.scs.2022.103796

[19] LUO Hai-ping, WANG Qing-zheng, GUAN Qing-yu, MA Yun-rui, NI Fei, YANG En-qi, ZHANG Jun. Heavy metal pollution levels, source apportionment and risk assessment in dust storms in key cities in Northwest China [J]. Journal of Hazardous Materials, 2022, 422(5): 126878. DOI: 10.1016/j.jhazmat. 2021.126878

[20] LIANG Jia-hui, LIU Zhao-yue, TIAN Yi-qi, SHI Hua-ding, FEI Yang, QI Jing-xian, MO Li. Research on health risk assessment of heavy metals in soil based on multi-factor source apportionment: A case study in Guangdong Province, China [J]. Science of the Total Environment, 2023, 858(3): 159991. DOI: 10.1016/j.scitotenv.2022.159991

[21] LI Xin-cheng, BING Jian-ping, ZHANG Jun-hong, GUO Li-quan, DENG Zhi-min, WANG Dang-wei, LIU Lin-shuang. Ecological risk assessment and sources identification of heavy metals in surface sediments of a river-reservoir system [J]. Science of the Total Environment, 2022, 842: 156683. DOI:10.1016/j. scitotenv.2022.156683

[22] JIANG Yan-xue, CHAO Si-hong, LIU Jian-wei, YANG Yue, CHEN Yan-jiao, ZHANG Ai-chen, CAO Hong-bin. Source apportionment and health risk assessment of heavy metals in soil for a township in Jiangsu Province, China [J]. Chemosphere, 2016, 168(2): 1658−1668. DOI: 10.1016/j.chemosphere.2016.11.088

[23] LIU Pen-feng, ZHENG Chao-jie, WEN Mei-lan, LUO Xian-rong, WU Zhi-qiang, LIU Ying-hong, CHAI She-li, HUANG Liang-liang. Ecological risk assessment and contamination history of heavy metals in the sediments of Chagan Lake, Northeast China [J]. Water, 2021, 13(7): 894. DOI:10.3390/w13070894

[24] LV Jian-shu, LIU Yang. An integrated approach to identify quantitative sources and hazardous areas of heavy metals in soils [J]. Science of the Total Environment, 2019, 646: 19−28. DOI: 10.1016/j.scitotenv.2018.07.257

[25] ZHANG Qi-fan, MENG Jing, SU Gui-jin, LIU Zhe-lu, SHI Bin, WANG Tie-yu. Source apportionment and risk assessment for polycyclic aromatic hydrocarbons in soils at a typical coking plant [J]. Ecotoxicology and Environmental Safety, 2021, 222: 112509. DIO: 10.1016/j.ecoenv.2021. 112509

[26] WANG Ling-qing, HAN Xiao-xiao, DING Shi-ming, LIANG Tao, ZHANG Yong-yong, XIAO Jun, DONG Lin-lin, ZHANG Hai-dong. Combining multiple methods for provenance discrimination based on rare earth element geochemistry in lake sediment [J]. Science of the Total Environment, 2019, 672: 264−274. DOI: 10.1016/j.scit otenv. 2019. 03.484

[27] PANDIT P, SAINI A, SAHU N, MEHRA R. Geochemical evaluation and environmental risk assessment of heavy metals: A case study from Ireland using Tellus stream sediment data (2011 — 2017) [J]. Groundwater for Sustainable Development, 2023, 23: 100974. DOI: 10.1016/j. gsd.2023.100974

[28] OTA Y, SUZUKI A, YAMAOKA K, NAGAO M, TANAKA Y, IRIZUKI T, FUJIWARA O, YOSHIOKA K, KAWAGATA S, KAWANO S, NISHIMURA O. Geochemical distribution of heavy metal elements and potential ecological risk assessment of Matsushima Bay sediments during 2012— 2016 [J]. Science of the Total Environment, 2020, 751: 141825. DOI:10.1016/j.scitotenv. 2020. 141825

[29] HU Bi-feng, JIA Xiao-lin, HU Jie, XU Dong-yun, XIA Fang, LI Yan. Assessment of heavy metal pollution and health risks in the soil-plant-human system in the Yangtze River Delta, China [J]. International Journal of Environmental Research & Public Health, 2017, 14(14): 14091042. DOI:10.3390/ ijerph14091042

[30] PENG Jing-yu, ZHANG Shuai, HAN Ying-yu, BATE Bate, KE Han, CHEN Yun-min. Soil heavy metal pollution of industrial legacies in China and health risk assessment [J]. Science of the Total Environment, 2022, 816: 151632. DOI: 10.1016/j.scitotenv.2021.151632

[31] LIN Yang, LUO Kai, SU Zi-lin, WU Yang, XIAO Wei, QIN Ming-xun, LIN Jing, ZHANG Shi-jie, ZHANG Yi, JIANG Yu-qi, PENG Bo-jin, GUO Yu-jing, WANG Xuan, Wang Yi-jun. Impact imposed by urbanization on soil heavy metal content of lake wetland and evaluation of ecological risks in East Dongting Lake in China [J]. Urban Climate, 2021, 42: 101117. DOI: 10.1016/j.uclim.2022.101117

[32] DU Yun, CAI Shu-ming, ZHANG Xiao-yang, ZHAO Yan. Interpretation of the environmental change of Dongting Lake, middle reach of Yangtze River, China, by ^{210}Pb measurement and satellite image analysis [J]. Geomorphology, 2001, 41(2/3): 171−181. DOI:10.1016/s0169-555x(01)00114-3

[33] WANG Ai-hua, HE Meng-chang, LIU Hui-ji, OUYANG Wei, LIU Xin-yi, LI Qin, LIN Chun-ye, LIU Xi-tao. Distribution heterogeneity of sediment bacterial community in the river-lake system impacted by nonferrous metal mines: Diversity, composition and co-occurrence patterns [J]. Environmental Pollution, 2023, 338: 122715. DIO: 10.1016/j. envpol.2023.122715

[34] GONG Jia-qiong, OUYANG Wei, HE Meng-chang, LIN Chun-ye. Heavy metal deposition dynamics under improved vegetation in the middle reach of the Yangtze River [J]. Environment International, 2023, 171: 107686. DOI: 10. 1016/j.envint.2022.107686

[35] LIU Zhao-yue, FEI Yang, SHI Hua-ding, MO Li, QI Jing-xian. Prediction of high-risk areas of soil heavy metal pollution with multiple factors on a large scale in industrial agglomeration areas [J]. Science of the Total Environment, 2022, 808: 151874. DOI: 10.1016/j.scitotenv. 2021. 151874

[36] MAKOKHA V A, QI Yue-ling, SHEN Yun, WANG Jun. Concentrations, distribution, and ecological risk assessment of heavy metals in the east Dongting and Honghu Lake, China [J]. Exposure and Health, 2016, 8(1): 31−41. DOI:10. 1007/s12403-015-0180-8

[37] DING Xian-wen, LI Xiao-feng. Monitoring of the water-area variations of Lake Dongting in China with ENVISAT ASAR images [J]. International Journal of Applied Earth Observation and Geoinformation, 2011, 13(6): 894−901. DOI: 10.1016/j.jag.2011.06.009

[38] CHAI Li-yuan, LI Huan, YANG Zhi-hui, MIN Xiao-bo, LIAO Qi, LIU Yi, MEN Shu-hui, YAN Ya-nan, XU Ji-xin. Heavy metals and metalloids in the surface sediments of the Xiangjiang River, Hunan, China: distribution, contamination, and ecological risk assessment [J]. Environmental Science & Pollution Research, 2016, 24: 874−885. DOI:10.1007/ s11356-016-7872-x

[39] LIU Hui-ji, ZENG Wei, HE Meng-chang, LIN Chun-ye, OUYANG Wei, LIU Xi-tao. Occurrence, distribution, and migration of antimony in the Zijiang River around a superlarge antimony deposit zone [J]. Environmental Pollution, 2023, 361(1): 120520. DIO: 10.1016/j. envpol. 2022.120520

[40] ZHANG Zhao-xue, LU Yi, LI Hai-pu, TU Yi, LIU Bo-yu, YANG Zhao-guang. Assessment of heavy metal contamination, distribution and source identification in the sediments from the Zijiang River, China [J]. Science of the Total Environment, 2018, 645(15): 235−243. DOI: 10.1016/ j.scitotenv.2018. 07.026

[41] FANG Xiao-hong, PENG Bo, SONG Zhao-liang, WU Si-cheng, CHEN Dan-ting, ZHAO Ya-fang, LIU Jing, DAI Ya-nan, TU Xiang-lin. Geochemistry of heavy metal-contaminated sediments from the Four River inlets of Dongting lake, China [J]. Environmental Science and Pollution Research, 2021, 28(10): 27593−27613. DOI:10. 1007/s11356-021-12635-0

[42] TONG Ting. Element concentrations in river delta sediments and mineral resources potential in the drainage watershed: A case study in the Xiangjiang, Zishui, Yuanjiang, and Lishui rivers watersheds [J]. Quaternary Sciences, 2005, 25(3): 298−305. (in Chinese). DOI: 10.3321/j.issn:1001-7410.2005. 03.005.

[43] LONG Xi-ting, LIU Fei, ZHOU Xin, PI Jing, YIN Wei, LI Fang, HUANG Shu-ping, MA Fang. Estimation of spatial distribution and health risk by arsenic and heavy metals in shallow groundwater around Dongting Lake Plain using GIS mapping [J]. Chemosphere, 2020, 269: 128698. DOI: 10.1016/j.chemosphere.2020. 128698

[44] FENG Yan, BAO Qian, XIAO Xiao, LIN Ma. Geo-accumulation vector model for evaluating the heavy metal pollution in the sediments of Western Dongting Lake [J]. Journal of Hydrology, 2019, 573: 40−48. DOI: 10. 1016/j.jhydrol.2019.03.064

[45] LIU Ling-ling, LIU Qi-yuan, MA Jin, Wu Hai-wen, Qu Ya-jing, GONG Yi-wei, YANG Shu-hui, AN Yan-fei, ZHOU Yong-zhang. Heavy metal(loid)s in the topsoil of urban parks in Beijing, China: Concentrations, potential sources, and risk assessment [J]. Environmental Pollution, 2020, 260: 114083. DOI: 10.1016/j.envpol.2020.114083

[46] LIU Juan, WANG Jin, XIAO Tang-fu, BAO Zhi-an, LIPPOLD H, LUO Xu-wen, YIN Mei-ling, REN Jia-min, CHEN Yong-heng, LINGHU W. Geochemical dispersal of thallium and accompanying metals in sediment profiles from a smelter-impacted area in South China [J]. Applied Geochemistry, 2018, 88(B): 239−246. DOI: 10.1016/j. apgeochem. 2017.05.013

[47] MÜLLER G. The heavy metal pollution of the sediments of the Neckar and its tributaries: An inventory [J]. Chemie in Unserer Zeit, 1981, 105: 157−64. (in German)

[48] USEPA. EPA Positive matrix factorization (PMF) 5.0 fundamentals and user guide [M]. U.S. Environment Protection Agency, Washington, 2014

[49] GUAN Qing-yu, WANG Fei-fei, XU Chuan-qi, PAN Ning-hui, LIN Jin-kuo, ZHAO Rui, YANG Yan-yan, LUO Hai-ping. Source apportionment of heavy metals in agricultural soil based on PMF: A case study in Hexi Corridor, northwest China [J]. Chemosphere, 2017, 193: 189−197. DOI: 10.1016/j.chemosphere.2017.10.151

[50] ZHANG Xiao-wen, WEI Shuai, SUN Qian-qian, WADOOD S A, GUO Bo-li. Source identification and spatial distribution of arsenic and heavy metals in agricultural soil around Hunan industrial estate by positive matrix factorization model, principle components analysis and geo statistical analysis [J]. Ecotoxicology and Environmental Safety, 2018, 159: 354−362. DOI:10.1016/j.ec oenv.2018. 04.072

[51] POLISSAR A V, HOPKE P K, PAATERO P. Atmospheric aerosol over Alaska: 2. Elemental composition and sources [J]. Journal of Geophysical Research Atmospheres, 1998, 103(15): 19045−19057. DOI:10.1029/98JD01212

[52] MEN Cong, LIU Rui-min, XU Li-bing, WANG Qing-rui, GUO Li-jia, MIAO Yue-xi, SHEN Zhen-yao. Source-specific ecological risk analysis and critical source identification of heavy metals in road dust in Beijing, China [J]. Journal of Hazardous Materials, 2019, 388: 121763. DOI: 10.1016/j. jhazmat.2019.121763

[53] HAKANSON L. An ecological risk index for aquatic pollution control. A sedimentological approach [J]. Water Research, 1980, 14(8): 975−1001. DOI:10.1016/0043-1354(80)90143-8

[54] HUANG Jing-ling, WU Yu-ying, SUN Jia-xun, LI Xiao, GENG Xiao-lei, ZHAO Meng-lu, SUN Ting, FAN Zheng-qiu. Health risk assessment of heavy metal(loid)s in park soils of the largest megacity in China by using Monte Carlo simulation coupled with Positive matrix factorization model [J]. Journal of Hazardous Materials, 2021, 415: 125629. DOI: 10.1016/j. jhazmat. 2021.125629

[55] LIN Yang, LUO Kai, SU Zi-lin, WU Yang, XIAO Wei, QIN Ming-xun, LIN Jing, ZHANG Shi-jie, ZHANG Yi, JIANG Yu-qi, PENG Bo-jin, GUO Yu-jing, WANG Xuan, WANG Yi-jun. Imposed by urbanization on soil heavy metal content of lake wetland and evaluation of ecological risks in East Dongting Lake [J]. Urban Climate, 2021, 42: 101117. DOI: 10.1016/j.uclim.2022.101117

[56] MCGRATH D, ZHANG Chao-sheng, CARTON O T. Geostatistical analyses and hazard assessment on soil lead in Silvermines area, Ireland [J]. Environmental Pollution, 2004, 127(2): 239−248. DOI: 10.1016/j.envpol.2003.07.002

[57] FU Sheng-yun, CHEN Jian-feng, LI Xiang-yu. Metallogenic regularity of mercury deposits in Hunan Province [J]. Geological Survey of China, 2017, 4(4): 17−25. (in Chinese). DOI: 10.19388/j.zgdzdc.2017.04.03

[58] YAO Yan, FENG Xin-bin, YAN Hai-yu, CHOU Guang-yue, SHANG Li-Hai, SHI Wen-fang. Mercury concentration in fish body in Hongjiadu reservoir of Guizhou province [J]. Chinese Journal of Ecology, 2010, 29(6): 1155−1160. (in Chinese) DOI: 10.13292/j.1000-4890.2010.0170

[59] LU Xin-wei, WANG Li-jun, LI L Y, LEI Kai, HUANG Li, KANG Dan. Multivariate statistical analysis of heavy metals in street dust of Baoji, NW China [J]. Journal of Hazardous Materials, 2010, 173(1/2/3): 744−749. DOI: 10.1016/j. jhazmat.2009.09.001

[60] SURESH G, RAMASAMY V, MEENAKSHISUNDARAM V, VENKATACHALAPATHY R, PONNUSAMY V. Influence of mineralogical and heavy metal composition on natural radionuclide concentrations in the river sediments [J]. Applied Radiation and Isotopes, 2011, 69(10): 1466−1474. DOI: 10.1016/ j.apradiso. 2011.05.020

[61] BROWN S G, EBERLY S, PAATERO P, NORRIS G A. Methods for estimating uncertainty in PMF solutions: Examples with ambient air and water quality data and guidance on reporting PMF results [J]. Science of the Total Environment, 2015, 518/519: 626−635. DOI: 10.1016/j. scitotenv.2015.01.022

[62] LIN Qi, LIU En-feng, ZHANG En-lou, LI Kai, SHEN Ji. Spatial distribution, contamination and ecological risk assessment of heavy metals in surface sediments of Erhai Lake, a large eutrophic plateau lake in southwest China [J]. Catena, 2016, 145: 193−203. DOI: 10.1016/j. catena.2016. 06.003

[63] ZHANG Meng, LI Xiao-ping, YANG Rui, WANG Ji-wen, AI Yu-wei, GAO Yu, ZHANG Yu-chao, ZHANG Xu, YAN Xiang-yang, LIU Bin, YU Hong-tao. Multipotential toxic metals accumulated in urban soil and street dust from Xining city, NW China: Spatial Occurrences, Sources, and Health Risks [J]. Archives of Environmental Contamination & Toxicology, 2019, 76(2): 308−330. DOI: 10.1007/s00244-018-00592-8

[64] MA Qiang, WANG Xue-qian, NING Ping, WANG Lang-lang, XU Bo-wen, CHEN Jun-hui, HUANG Jia-yan,

HE Ji-ming. Status of atmospheric thallium pollution and research progress of treatment technology [J]. Environmental Chemistry, 2020, 39(12): 3362−3370. (in Chinese). DOI: 10.7524/j.issn.0254-6108.2020042801

[65] FANG Xiao-hong, PENG Bo, WANG Xin, SONG Zhao-liang, ZHOU Dong-xiao, WANG Qin, QIN Zhi-lian, TAN Chang-yin. Distribution, contamination and source identification of heavy metals in bed sediments from the lower reaches of the Xiangjiang River in Hunan province, China [J]. Science of the Total Environment, 2019, 689(1): 557−570. DOI: 10.1016/j.scitotenv. 2019.06.330

[66] ZHU Hui-na, YUAN Xing-zhong, ZENG Guang-ming, JIANG Min, LIANG Jie, ZHANG Chang, YIN Juan, HUANG Hua-jun, LIU Zhi-feng, JIANG Hong-wei. Ecological risk assessment of heavy metals in sediments of Xiawan Port based on modified potential ecological risk index [J]. Transactions of Nonferrous Metals Society of China, 2012, 22: 1470−1477. DOI: 10.1016/ S1003-6326(11) 61343-5

[67] ZHU Qing-qing, WANG Zhong-liang. Distribution characteristics and source analysis of heavy metals in sediments of the main river systems in China [J]. Earth and Environment, 2012, 40(3): 305−313. (in Chinese). DOI: 10.14050/j.cnki.1672-9250.2012.03.001

[68] GUO Zhao-hui, SONG Jie, XIAO Xi-yuan, MING Hui, MIAO Xu-feng, WANG Feng-yong. Spatial distribution and environmental characterization of sediment-associated metals from middle-downstream of Xiangjiang River, southern China [J]. Journal of Central South University, 2010, 17(1): 68−78. DOI: 10.1007/s11771-010-0013-7

[69] QI Jian-ying, ZHANG Hai-long, LI Xiang-ping, LU Jian, ZHANG Gao-sheng. Concentrations, spatial distribution, and risk assessment of soil heavy metals in a Zn−Pb mine district in southern China [J]. Environ Monit Assess, 2016, 188: 1−11. DOI: 10.1007/s10661-016-5406-0

[70] PENG Yi-zhe, HUANG Feng-lian, JIANG Ping-hong, LUO Lin, YANG Yuan, PENG Ke-jian. Research on discharge control of thallium pollutants from hunan industrial wastewater based on the environmental capacity of surface water [J]. Ecology and Environmental Sciences, 2020, 29(10): 2070−2080. (in Chinese). DOI: 10.16258/j.cnki. 1674-5906.2020.10.018

[71] HU Ying, Qi Shi-hua, Wu Chen-xi, KE Yan-ping, CHEN Jing, CHEN Wei, GONG Xiang-yi. Preliminary assessment of heavy metal contamination in surface water and sediments from Honghu Lake, East Central China [J]. Frontiers of Earth Science, 2012, 6(1): 39−47. DOI:10.1007/s11707-012-0309-z

[72] JIANG Xiao-liang, XIONG Zi-qian, LIU Hui, LIU Gui-hua, LIU Wen-zhi. Distribution, source identification, and ecological risk assessment of heavy metals in wetland soils of a river-reservoir system [J]. Environmental Science and Pollution Research, 2016, 24: 436−444. DOI: 10.1007/ s11356-016-7775-x

[73] LI He, WANG Shu-hang, CHE Fei-fei, JIANG Xia, NIU Yong. Mate analysis of heavy metal pollution in sediments of Chaohu Lake, Dongting Lake and Poyang Lake [J]. China Environmental Science, 2023, 43(2): 831−842. (in Chinese). DOI: 10.19674/j.cnki.issn1000-6923.20221115.001

[74] LI Jun, LI Xu, LI Kai-ming, JIAO Liang, TAI Xi-sheng, CANG Fei, CHEN Wei, TUO Xin-yin. Identification priority source of heavy metals pollution in greenspace soils based on source-specific ecological and human health risk analysis in the Yellow River custom tourist line of Lanzhou [J]. Environmental Science, 2024, 45(4): 2428−2439. (in Chinese). DOI: 10.13227/j.hjkx. 202304165

洞庭湖表层沉积物中重金属的空间特征及特定源生态风险评价

周 瑶[1,2,3]，成永生[1,2,3]

1. 中南大学 有色金属成矿预测与地质环境监测教育部重点实验室，长沙 410083；
2. 有色资源与地质灾害探查湖南省重点实验室，长沙 410083；
3. 中南大学 地球科学与信息物理学院，长沙 410083

摘 要：重金属污染导致的环境问题备受世界关注。精准识别重金属污染来源以及定量评价其生态风险对重金属污染防控至关重要。以中国第二大淡水湖的洞庭湖为例，结合正定矩阵因子分解(PMF)源解析以及综合生态风险评价(NIRI)等方法，研究了洞庭湖浅层沉积物中 14 种重金属的空间分布、污染特征、污染来源及各污染源和污染物对区域生态风险的贡献。结果表明，研究区重金属的含量平均值是相应背景值的 0.82~9.44 倍。重金属空间分布特征差异明显，As、Cd、Mn、Pb、Sn、Tl 和 Zn 含量高值区集中分布在湘江和长江采样带；Co、Cr、Cu、Ni 和 V 含量高值区集中分布在澧水采样带；Hg 和 Sb 的高值点分别集中分布在沅江采样带和资水采样带。重金属积累受汞矿开采和大气沉降(F1)(17.99%)、城市生活污水和工业污水(F2)(24.44%)、锑矿采选与冶炼源(F3)(6.50%)、有色金属采选与延展加工类工业源(F4)(15.72%)和以天然源和农业源为主的混合源(F5)(35.35%)的影响，其中 F1 和 F2 为主要污染源。Cd、Hg、Tl、Sb 和 As，尤其 Cd 和 Hg，存在较高的生态风险，为优先控制污染元素。

关键词：洞庭湖；表层沉积物；重金属污染；源解析；PMF 模型；风险评价

(Edited by Bing YANG)